Inorganic Chemistry
Article

Inorg. Chem. **2009**, *48*, 10397–10404 **10397**
DOI: 10.1021/ic900875b

Tight-Contact Ion Pairs Involving Pt(II) Dithiooxamide Complexes: the Acid−Base Reactions between Hydrohalogenated Ion-Paired Complexes and Pyridine

Antonino Giannetto,*,† Fausto Puntoriero,† Anna Barattucci,‡ Santo Lanza,*,† and Sebastiano Campagna*,†

†*Dipartimento di Chimica Inorganica, Chimica Analitica e Chimica Fisica, Università di Messina, Via Sperone 31, 98166 Messina, Italy, and* ‡*Dipartimento di Chimica Organica e Biologica, Università di Messina, Via Sperone 31, 98166 Messina, Italy*

Received May 6, 2009

The equilibrium constants relative to HCl exchange between Pt(II)-containing tight contact ion pairs (TCIP) and pyridine have been investigated in chloroform solution at 298 K. The general formulas of the metal species are: $\{[Pt(H_2\text{-}R_2\text{-dithiooxamide})_2]^{2+}, 2Cl^-\}$ (**a-**type compounds; R=methyl (**1a**), ethyl (**2a**), *n*-propyl (**3a**), iso-propyl (**4a**), *n*-butyl (**5a**), cyclohexyl (**6a**), benzyl (**7a**), β-phenyl-ethyl (**8a**), allyl (**9a**)) and $\{[(H\text{-}R_2\text{-dithiooxamidate})Pt(H_2\text{-}R_2\text{-dithiooxamide})]^+, Cl^-\}$ (**b**-type compounds; R has the same meanings as before, given rise to **1b**−**9b** species; moreover, the mixed R compound **10b**, containing R=benzyl on a DTO (dthiooxamidate/dithiooxamide) ligand and R = ethyl on the other DTO ligand, has also been investigated). Moreover, the parent species $[Pt(H\text{-}R_2\text{-dithiooxamidate})_2]$ (**c-**type compounds; **1c**−**10c**) have also been prepared. Out of 29 compounds reported in the paper, 19 compounds are here reported for the first time, and their synthesis and characterization data are also given. Compounds of **a**-type exhibit two successive equilibrium constants, which are related to successive HCl transfer from the TCIP to pyridine. By comparing the equilibrium constants Kc of the various **b-**type species, we have been able to (i) obtain information on the relative stability of the TCIP and, by taking advantage of the two equilibrium constants Kc1 and Kc2 found for each **a**-type species, (ii) gain knowledge on the electronic interaction between the two basic sites of the Pt(II) bis-dithiooxamide complexes, mediated by the metal center. Linear relationships are found between the pKc of the compounds and the σ-Taft value ($\Sigma\sigma^*$) of the amine substituents of the DTO ligands. Interestingly, the slope of such linear correlations is much steeper for pKc2 than for pKc1, indicating that the electronic interaction between the basic sites increases with the electron donating ability of the R substituent. A parallel is proposed between the splitting of HCl transfer equilibrium constants in **a**-type TCIP and oxidation potential splitting in dinuclear, bridge-linked metal complexes.

Introduction

Tight-contact ion pairs (TCIPs) play key roles in anion and ion-pair receptor chemistry,[1,2] and in general in the functional behavior of most cofactors and substrates involved in biological transformations and/or processes, which are usually anionic in nature.[3,4] An example of biological processes involving TCIPs is potassium transport in biological membranes, which is supposed to be mediated by the formation of weak ion pairs.[5] The formation of TCIP also plays important roles on processes involving artificial systems, like the stabilization of some diacids[6] and the anion-templated assembly of catenanes and pseudorotaxanes.[7] However, in spite of the importance of TCIPs in the above-mentioned fields, detailed investigations on the parameters which determine TCIP formation and stability are quite rare, in particular when multiple TCIP equilibria are involved.

*To whom correspondence should be addressed. E-mail: giannettoa@unime.it (A.G.), lanza@unime.it (S.L.), campagna@unime.it (S.C.).

(1) (a) Beer, P. D.; Gale, P. A. *Angew. Chem., Int. Ed.* **2001**, *40*, 486. (b) Gale, P. A. *Coord. Chem. Rev.* **2003**, *240*, 191. (c) Sessler, J. L.; Gale, P. A.; Cho, W.-S. *Anion Receptor Chemistry*; Royal Society of Chemistry: Cambridge, 2006.

(2) (a) Manabe, K.; Okamura, K.; Date, T.; Koga, K. *J. Org. Chem.* **1993**, *58*, 6692. (b) Motomura, T.; Aoyama, Y. *J. Org. Chem.* **1991**, *56*, 7224. (c) Reetz, M. T.; Niemeyer, C. M.; Hermes, M.; Goddard, R. *Angew. Chem., Int. Ed.* **1992**, *31*, 1017. (d) Dietrich, B.; Hosseini, M. W.; Lehn, J.-M.; Sessions, R. B. *J. Am. Chem. Soc.* **1981**, *103*, 1282. (e) Dixon, R. P.; Geib, S. J.; Hamilton, A. D. *J. Am. Chem. Soc.* **1992**, *114*, 365. (f) Ariga, K.; Anslyn, E. V. *J. Org. Chem.* **1992**, *57*, 417. (g) Arduini, A.; Secchi, A.; Pochini, A. In *Calyxarenes in the Nanoworld*; Vicens, J., Harrowfield, J., Eds.; Springer: Berlin, 2007; p 63, and refs. therein

(3) Yoon, D.-W.; Gross, D. E.; Lynch, V. M.; Lee, C.-H.; Bennett, P. C.; Sessler, J. L. *Chem. Commun.* **2009**, 1109, and refs. therein.

(4) (a) Jeffrey, G. A.; Saenger, W. *Hydrogen Bonding in Biological Structures*; Springer-Verlag: Berlin, 1991. (b) Hughes, M. P.; Smith, B. D. *J. Org. Chem.* **1997**, *62*, 4492.

(5) (a) Gadsby, D. C. *Nature* **2004**, *427*, 795–7. (b) Noskov, S. Y.; Bernèche, S.; Roux, B. *Nature* **2004**, *431*, 830.

(6) Karaman, R.; Bruice, T. C. *Inorg. Chem.* **1992**, *31*, 2455.

(7) (a) Sambrook, M. R.; Beer, P. D.; Wisner, J. A.; Paul, R. L; Cowley, A. R. *J. Am. Chem. Soc.* **2004**, *126*, 15364. (b) Sambrook, M. R.; Beer, P. D.; Wisner, J. A.; Paul, R. L; Cowley, A. R.; Szemes, F.; Drew, M. G. B. *J. Am. Chem. Soc.* **2005**, *127*, 2292.

Published on Web 10/02/2009

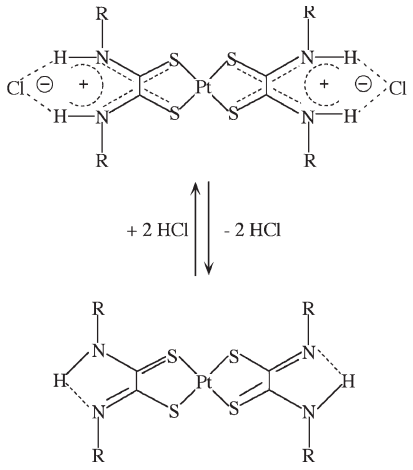

Figure 1. Schematization of the equilibrium between TCIP and dehydrohalogenated species.

Recently, we have demonstrated the ability of [Pt(H-R_2-dithiooxamidate)$_2$] complexes (R = alkyl groups) to form TCIPs of general formula {[Pt(H_2-R_2-dithiooxamide)$_2$]$^{2+}$, 2Cl$^-$} (see Figure 1) by addition of HCl,[8,9] where ion-pair formation is driven by H-bonding. The process is common to HX species, where X is a halogen or a pseudo-halogen anion.[9] Moreover, we have also reported that new solid-state luminescent sensors for gaseous HCl or amines can be prepared by taking advantage of the luminescent nature of the {[Pt(H_2-R_2-dithiooxamide)$_2$]$^{2+}$, 2Cl$^-$} species as opposed to the absence of luminescence of the corresponding neutral [Pt(H-R_2-dithiooxamidate)$_2$] complexes. Such luminescent sensors operate via switchable formation of TCIP species,[10] an extension of our former solution studies on the photophysical properties of Pt(II) dithiooxamide/dithiooxamidate compounds.[9,11]

To gain information on the equilibrium between TCIPs containing HCl "moieties" and parent dehydrohalogenated systems in Pt(II) bis(R-dithiooxamide/amidate) complexes, so inferring useful concepts for the design of more elaborate luminescent sensors and, on a broader viewpoint, to learn more on parameters capable to influence TCIP stability, we started a systematic investigation on the properties which govern the equilibrium shown in Figure 1. In particular, here we investigate the equilibrium constants between {[Pt(H_2-R_2-dithiooxamide)$_2$]$^{2+}$, 2Cl$^-$} and pyridine in chloroform solution. Indeed, pyridine can compete with {([Pt(H_2-R_2-dithiooxamide)$_2$])$^{2+}$, 2Cl$^-$} species for protons, so driving formation of the neutral parent complexes from the tight ion pairs. The reactions studied are shown in eqs 1 and 2. In these equations, py stands for pyridine and DTO stands for dithiooxamidate or dithiooxamide ligands. By comparing the equilibrium constants for such reactions in the various compounds, we have been able to (i) obtain information on the relative stability of the TCIP, and, by taking advantage of the difference between the two equilibrium constants involving sequential titration of the two HCl moieties in each compound, (ii) gain knowledge on the electronic interaction between the two basic sites of the Pt(II) bis-dithiooxamide complexes, mediated by the metal center. The investigation has been performed by analyzing the properties of 29 complexes (see Figure 2 for structural formulas): 19 are new species, whose synthesis and full characterization is here reported. Among the compounds (see Figure 2), nine contain two HCl "complexed" sites (type **a** species), 10 are neutral species (type **c** species), and 10 are mixed systems (type **b** species). Also two compounds containing different R substituents have been investigated (**10b** and **10c**).

$$\{[Pt(H_2\text{-}R_2\text{-}DTO)_2]^{2+}, 2Cl^-\} + py \rightleftharpoons \{[(H\text{-}R_2\text{-}DTO)Pt(H_2\text{-}R_2\text{-}DTO)]^+, Cl^-\} + py\cdot HCl \quad (1)$$

$$\{[(H\text{-}R_2\text{-}DTO)Pt(H_2\text{-}R_2\text{-}DTO)]^+, Cl^-\} + py \rightleftharpoons [Pt(H\text{-}R_2\text{-}DTO)_2] + py\cdot HCl \quad (2)$$

Results and Discussion

Synthetic Approach and Structural Considerations. TCIPs **1a**−**9a** can be easily obtained in very high yields by adding the 2-fold amount of the desired substituted dithiooxamide species to *cis*-Pt(Me_2SO)$_2$Cl$_2$ (Scheme 1, step i) in chloroform.[8,9] The neutral complexes **1c**−**9c** are prepared from **1a**−**9a** ion pairs by adding sodium bicarbonate (step ii in Scheme 1). Although the formation of TCIPs **1a**−**9a** is a stepwise process, the monochelate ion pairs {[(Me_2SO)ClPt(H_2-R_2-DTO)]$^+$,Cl$^-$} are not stable in solution.[8] However, the addition of the stoichiometric amount of the desired dithiooxamide to a chloroform suspension of *cis*-Pt(Me_2SO)$_2$Cl$_2$ in the presence of sodium bicarbonate affords the stable monochelate complexes [(Me_2SO)ClPt(H-R_2-DTO)] (Scheme 1, step iii). Such monochelate complexes have been already synthesized and fully characterized,[12] but here they have not been isolated in that they were used as intermediate species toward the preparation of **b**-type species. Indeed, after removing sodium bicarbonate, a further stoichiometric amount of substituted dithioxamide is added to the solution obtained by step iii, to finally yield type-**b** complex ion pairs {[(H-R_2-DTO)Pt(H_2-R_2-DTO)]$^+$,Cl$^-$} in a high yield (Scheme 1, step iv). Dehydrohalogenation of **b**-type ion pairs provides **c**-type complexes (Scheme 1, step v). If a different dithioxamide H_2-R′$_2$-DTO is added to [(Me_2SO)ClPt(H-R_2-DTO)] in step iv, compounds having different R substituents can be obtained. This is the route used for preparing **10b** and **10c**.

Type **c** complexes exhibit a planar structure.[8] On the contrary, the bis-chelated **a**-type complexes cannot have a planar asset of dithiooxamide ligands around the square planar Pt(II) center since two coplanar amidic hydrogens would exert a high reciprocal repulsion, and as a consequence the dithooxamide ligands have to be distorted

(8) Rosace, G.; Bruno, G.; Monsù Scolaro, L.; Nicolò, F.; Sergi, S.; Lanza, S. *Inorg. Chim. Acta* **1993**, *208*, 59.
(9) Rosace, G.; Giuffrida, G.; Guglielmo, G.; Campagna, S.; Lanza, S. *Inorg. Chem.* **1996**, *35*, 6816.
(10) Nastasi, F.; Puntoriero, F.; Palmeri, N.; Cavallaro, S.; Campagna, S.; Lanza, S. *Chem. Commun.* **2007**, 4740.
(11) For other cases of photophysical properties of TCIPs, see for example: McCosar, B. H.; Schanze, K. S. *Inorg. Chem.* **1996**, *35*, 6800.
(12) Lanza, S.; Loiseau, F.; Tresoldi, G.; Serroni, S.; Campagna, S. *Inorg. Chim. Acta* **2007**, *360*, 1929.

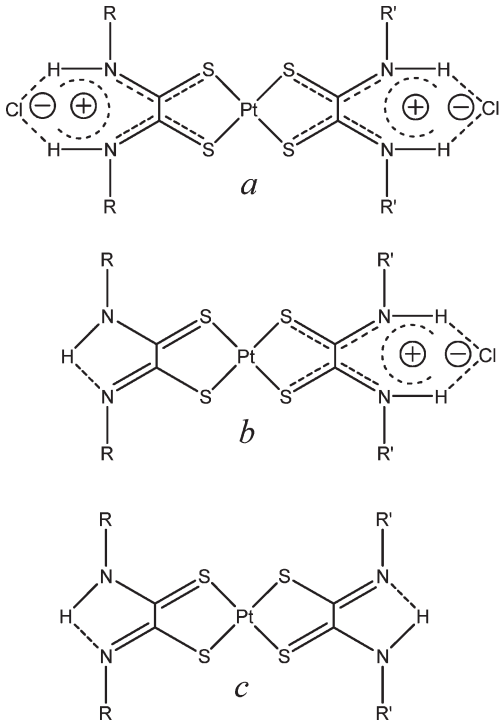

R = R' = Methyl ***1a, 1b,1c***

R = R' = Ethyl ***2a, 2b,2c***

R = R' = *n*propyl ***3a, 3b,3c***

R = R' = isopropyl ***4a, 4b,4c***

R = R' = *n*butyl ***5a, 5b,5c***

R = R' = Cyclohexyl ***6a, 6b,6c***

R = R' = Benzyl ***7a, 7b,7c***

R = R' = β-phenylethyl ***8a, 8b,8c***

R = R' = Allyl ***9a, 9b,9c***

R = Benzyl, R' = ethyl ***10b,10c***

Figure 2. Structural formulas and abbreviations of the investigated complexes.

Scheme 1. Synthetic Routes for **a**-, **b**-, and **c**-Type Complexes

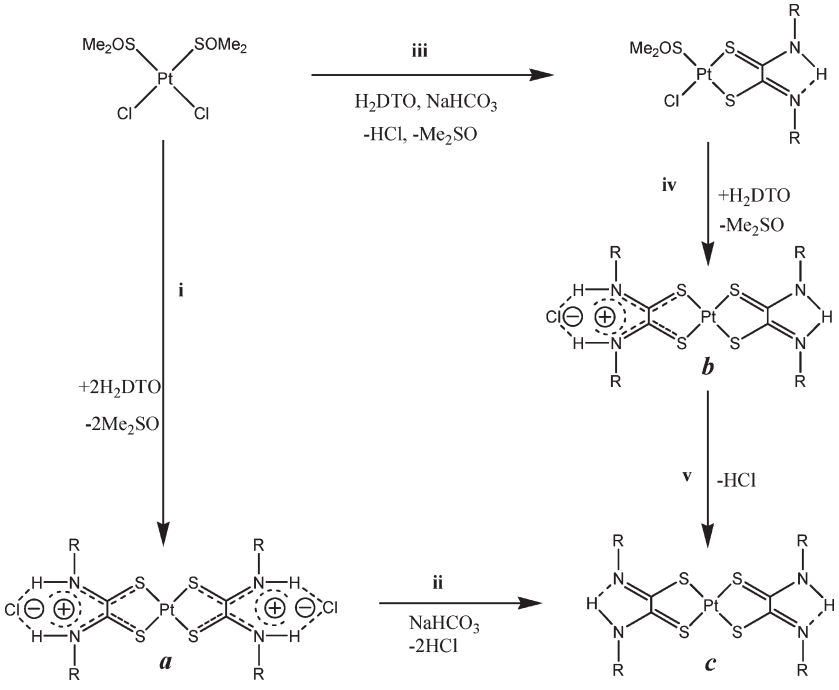

from planarity. Actually, the crystal structures of neutral dithiooxamide complexes of copper, zinc,[13] and bismuth[14] show R(H)NC(=S)-C(=S)N(H)R torsional angles of about 45°. Nevertheless, **a**-type complexes exhibit sharp A_2 or A_2B_2 signals for N−CH_2− protons, and this suggests the rapid twisting of R(H)NC(=S) groups around the C−C pivot bond of the S,S-coordinated dithiooxamide. Type **b** complexes are constituted by a S,S-chelate dithiooxamidate and a S,S chelate dithiooxamide which retains a chloride ion as a contact ion pair. However, their proton spectra in solution show only one pattern of signals for identical R groups of both S,S-chelate ligands; this is in line with a rapid intermolecular exchange of the HCl moiety between the nitrogen systems of the ligands.

(13) Antolini, L.; Fabretti, G.; Franchini, L.; Menabue, G.; Pellacani, C.; Desseyn, H. O.; Dommisse, R.; Hoffamans, H. C. *J. Chem. Soc., Dalton Trans.* **1987**, 1921.

(14) Drew, M. G. B.; Kisenyi, J. M.; Willey, G. R. *J. Chem. Soc., Dalton Trans.* **1984**, 1723.

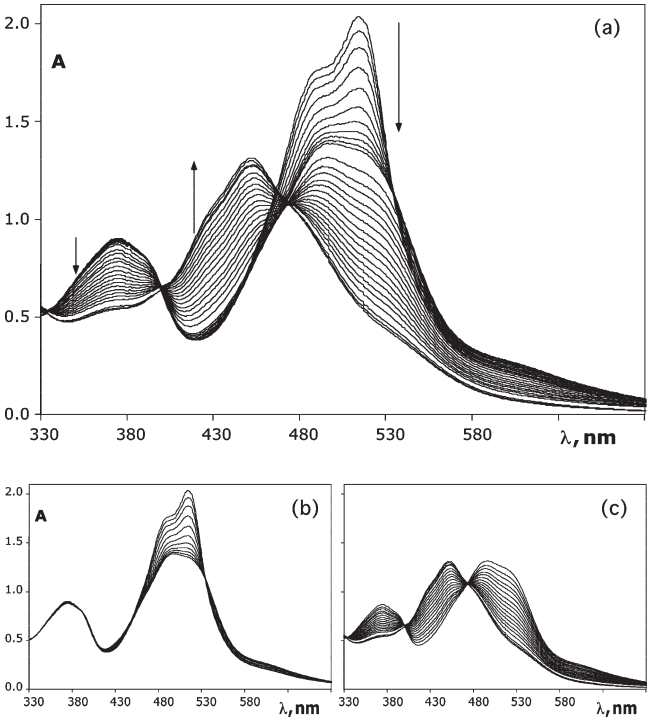

Figure 3. Changes of the absorption spectrum of **4a** (1.39×10^{-4} M) upon successive pyridine addition in chloroform. Panel (a) shows the overall process, and panels (b) and (c) show the separate two successive processes. See text for details.

Acid−Base Behavior. Pyridine has been successfully used to study proton transfer.[15] Since proton transfer is the first requisite for the occurrence of the equilibria shown in eqs 1 and 2, we performed titration of such equilibria by using pyridine as the titration agent for the $\{[Pt(H_2\text{-}R_2\text{-}DTO)_2]^{2+}, 2Cl^-\}$ complexes (**1a**−**9a**) in chloroform, by following the evolution of the process spectrophotometrically.

A typical experiment is shown in Figure 3, reporting the changes of the absorption spectrum of $\{[Pt(H_2\text{-}(iso\text{-}propyl)_2\text{-}DTO)_2]^{2+}, 2Cl^-\}$ (**4a**) upon pyridine addition. Clearly, two successive reactions take place, and each one is characterized by a set of isosbestic points. For **4a**, isosbestic points are at 533 and 446 nm for the first step, whereas isosbestic points for the second step are at 471 and 401 nm. Figure 4 shows the titration curves connected with the experiment in Figure 3. All the **a**-type complexes exhibit similar absorption spectrum changes and titration behavior, which corresponds to sequential HCl transfer from the Pt(II) complexes to pyridines. This assignment is confirmed by comparison of the spectra obtained upon first and second titration steps of the **a**-type compounds with those of the corresponding **b**-type and **c**-type compounds, independently prepared (compare spectra in Figure 3 with those shown in Supporting Information). The absorption spectra changes upon pyridine titration have already been interpreted[9,10] and are due to a blue-shift of the low-energy charge-transfer (CT) band, corresponding to a CT transition from a Pt/S orbital to DTO-centered orbitals, on passing from **a**-type to **c**-type species.

(15) See for example: Menger, F. M.; Singh, T. D.; Bayer, F. L. *J. Am. Chem. Soc.* **1976**, *98*, 5011.

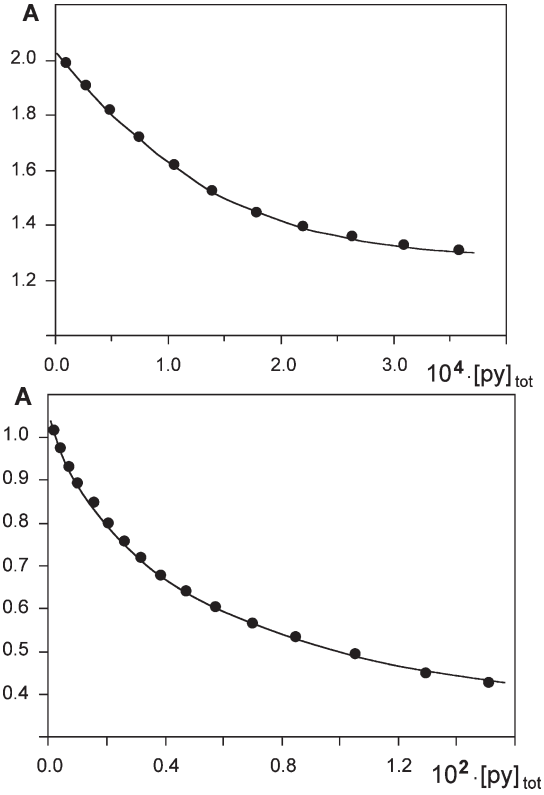

Figure 4. Titration curves relative to the experiments in Figure 3(b) (top) and Figure 3(c) (bottom). [complex] = 1.39×10^{-4} M. Top: absorption values monitored at $\lambda = 513$ nm; bottom: absorption values monitored at $\lambda = 534$ nm. [py] stands for molar concentration of added pyridine. A stands for absorbance.

Table 1. Equilibrium Constants and σ-Taft Values[a]

compound	R substituent	Kc1	Kc2	$\Sigma\sigma^*$	pKc1	pKc2
1a	methyl	4.1 (±0.4)	0.066 (±0.004)	−0.98	−0.613	1.180
2a	ethyl	2.3 (±0.4)	0.039 (±0.003)	−0.88	−0.362	1.409
3a	*n*-propyl	2.2 (±0.3)	0.077 (±0.05)	−0.86	−0.342	1.113
4a	iso-propyl	1.7 (±0.2)	0.028 (±0.003)	−0.79	−0.230	1.796
5a	cyclohexyl	2.6 (±0.3)	0.024 (±0.002)	−0.83	−0.415	1.620
6a	*n*-butile	2.1 (±0.3)	0.062 (±0.004)	−0.85	−0.322	1.208
7a	benzyl	7.2 (±0.5)	1.280 (±0.05)	−1.20	−0.857	−0.107
8a	*β*-phenyl-ethyl	4.9 (±0.5)	0.250 (±0.05)	−1.06	−0.690	0.602
9a	allyl	6.1 (±0.5)	1.40 (±0.05)	−1.11	−0.785	−0.146
10b[b]	benzyl/ethyl		0.150 (±0.005)	−1.03		0.824

[a] Data are in chloroform solution at 298 K. $\Sigma\sigma^*$ values are taken from ref 16b, and refer to the value derived from the amine species used to prepare the **a**-type compounds (see ref 17). The Kc2 values of the **a**-type compounds are identical, within experimental uncertainty, to the single Kc value obtained for the corresponding **b**-type compounds. [b] The Kc2 value for **10b** is the single Kc value obtained. The $\Sigma\sigma^*$ value assigned to this compound has a different meaning, explained in the text.

The equilibrium constants Kc are collected in Table 1, which also reports the pKc values. The different Kc constants (Kc1 and Kc2, see eqs 3 and 4, related to equilibria in eqs 1 and 2, respectively) of the two titration equilibria for each compound indicate that significant electronic interaction takes place between the two sites involved in equilibrium reactions. The equilibrium in eq 2 has also been investigated by using the independently prepared and characterized $\{[(H\text{-}R_2\text{-}DTO)Pt(H_2\text{-}R_2\text{-}DTO)]^+, Cl^-\}$

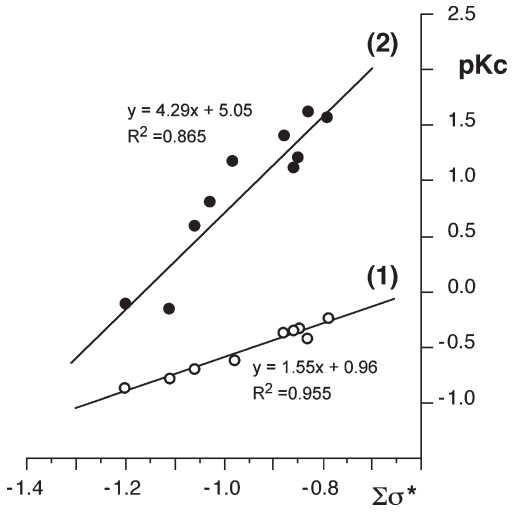

Figure 5. Plots of pKc vs $\Sigma\sigma^*$ values given in Table 1; (1) and (2) refer to pKc1 and pKc2, respectively.

b-type species. Obviously, for the **b**-type species (which only contain a single acid site) a single titration step was found, and the Kc values obtained (not shown) are identical, within experimental uncertainty, to the Kc2 values of the corresponding type-**a** species. An exception to this general trend is represented by **10b**, whose behavior will be discussed later.

$$\mathrm{Kc1} = \frac{[\{[(\text{H-R}_2\text{-DTO})\mathrm{Pt}(\text{H}_2\text{-R}_2\text{-DTO})]^+, \mathrm{Cl}^-\}][\mathrm{pyHCl}]}{[\{[\mathrm{Pt}(\text{H}_2\text{-R}_2\text{-DTO})_2]^{2+}, 2\mathrm{Cl}^-\}][\mathrm{py}]} \quad (3)$$

$$\mathrm{Kc2} = \frac{[\mathrm{Pt}(\text{H-R}_2\text{-DTO})_2][\mathrm{pyHCl}]}{[\{[(\text{H-R}_2\text{-DTO})\mathrm{Pt}(\text{H}_2\text{-R}_2\text{-DTO})_2]^+, \mathrm{Cl}^-\}][\mathrm{py}]} \quad (4)$$

The data in Table 1 warrant extensive discussion. The Kc values are related to the stability of the $\{[\mathrm{Pt}(\text{H}_2\text{-R}_2\text{-DTO})_2]^{2+}, 2\mathrm{Cl}^-\}$ ion pairs: at a first approximation, lower values indicate that the equilibria in eqs 1 and 2 are displaced toward the reactants, suggesting an increased relative stability of the $\{[\mathrm{Pt}(\text{R-DTO})_2\text{H}_2]^{2+}, 2\mathrm{Cl}^-\}$ ion pair. A very good linear correlation is found between the pKc values and the so-called σ-Taft value ($\Sigma\sigma^*$)[16,17] of the amine substituents of the DTO ligands (Figure 5).

The σ-Taft value for an amine is a constant which expresses the polar effect of the substituents, taking also into account for steric effects on the nitrogen atom, so determining its basicity. In other words, the σ-Taft value reflects the effective electron density on the nitrogen atom. In our case, it expresses the ability of the DTO ligands to coordinate protons (and, via hydrogen bonding, the HCl "moiety"). It is therefore not unexpected that the linear correlation in Figure 5 is found, with less negative $\Sigma\sigma^*$ values corresponding to higher effective electron density on the nitrogen and as a consequence to lower pKc values, that is, relatively more stable TCIPs.

The second equilibrium constants Kc2 values span a much larger range for the series of compounds under study, compared to the first equilibrium constants Kc1 values (Table 1, Figure 5), although the linear correlation between Kc2 and the Taft constant is still kept. Differences between Kc1 and Kc2 for each species are related to the electronic interaction between the two active sites. Apparently, the difference in Kc1 and Kc2 increases with the electronic density on the nitrogen of the amine substituents of the DTO, as indicated by the Taft constant. Such a behavior can be rationalized by considering that upon the first step of the titration (that is, once **b**-type species are formed from **a**-type compounds), the electron density on the already titrated nitrogen, which is not engaged in hydrogen bonding anymore, is now available to be partially transferred, via the Pt(II) complex molecular framework, to the other half of the molecule where the hydrogen bonding is still present, reinforcing the still existing TCIP. Such a reinforcement effect is therefore more effective (so leading to a larger splitting in the Kc values) for R substituents inducing more effective electron density on their nitrogens, according to the σ-Taft values. The situation is reminiscent of the oxidation splitting occurring in symmetric dinuclear metal complexes where the metal centers, which undergo oxidation, are connected by bridging ligands.[18] In these latter species, oxidation of the first metal center causes a shift of electron density, via bridging ligand orbitals, making second metal oxidation more difficult. When the bridging ligand is kept constant, the metal-centered oxidation splitting depends on the effective electron density which is located on each metal center (in other words, from the energy level of the metal-centered occupied orbitals), on its turn a function of the nature of the peripheral ligands. For strongly electron acceptors peripheral ligands, leaving less electron density on the metal centers (i.e., strongly stabilizing the metal orbitals, which have to couple with the lowest unoccupied molecular orbital (LUMO) centered in the bridging ligands, in the superexchange electron-transfer mechanism mediating the metal−metal coupling), oxidation splitting can not occur.[19,20] In this similitude, oxidation splitting is here represented by Kc1 and Kc2 splitting and the electronic factors, governed in bridged dinuclear metal complexes by peripheral ligands, are here determined by the σ-Taft values of the nitrogen substituents of the dithiooxamide ligands. As a matter of fact, Kc1 and Kc2 tend to become closer and closer with decreasing σ-Taft values, and can be predicted that for

(16) (a) Taft, R. W. *J. Am. Chem. Soc.* **1953**, *75*, 4231. (b) Hall, H. K., Jr. *J. Am. Chem. Soc.* **1957**, *79*, 5441. (c) De Tar, D. F. *J. Am. Chem. Soc.* **1980**, *102*, 7988.

(17) As $\Sigma\sigma^*$ values, we used the values reported in ref 16b for the various amines. Note that we used the values for the amines employed to prepare the DTO ligands, and not the $\Sigma\sigma^*$ of the DTO ligands, which should be used from a more rigorous point of view. However, we feel that this functional approximation is acceptable, since the difference in the DTO properties are dictated by the R substituents on the nitrogens.

(18) (a) Robin, M. B.; Day, P. *Adv. Inorg. Radiochem.* **1967**, *10*, 247. (b) Richardson, D. E.; Taube, H. *J. Am. Chem. Soc.* **1983**, *105*, 40. (c) Creutz, C. *Prog. Inorg. Chem.* **1983**, *30*, 1.

(19) Giuffrida, G.; Campagna, S. *Coord. Chem. Rev.* **1994**, *135*−*136*, 517.

(20) The situation is even more general. This discussion applies indeed to any symmetric species with two identical redox-active sites, and has its explanation in the superexchange theory.[21] The dinuclear metal complexes oxidation splitting is taken as an example, and a simplified view is here used for immediate qualitative comparison with the present systems.

nitrogen substituents yielding σ-Taft values of about -1.45, a single titration process, corresponding to simultaneous transfer of the two HCl moieties of a $\{[Pt(H_2\text{-}R_2\text{-}DTO)_2]^{2+}, 2Cl^-\}$ species to pyridines, can take place.

As already mentioned, **10b** represents a unique species in the series of compounds here studied: it is a monohydrohalogenated species containing differently N-substituted DTO moieties (Figure 2). Whereas for the other **b**-type species here studied, which all have identical N-substituted DTO moieties on both sides of the metal complex, the coordinated HCl molecule is very rapidly exchanged between the two sites, the N-substituted DTO species of **10b** have quite different basic properties (compare Kc values of **2a** and **7a** in Table 1), so that the coordinated HCl can become prevalently localized on the (more basic) ethyl-substituted DTO. The single Kc value obtained for **10b** (reported in Table 1 as Kc2, for uniformity of presentation) is therefore most likely referred to the titration of HCl moiety coordinated by the ethyl-substituted DTO. Within such an assumption, if no electronic interaction was active between the two DTO moieties of the complex, the Kc value for **10b** should correspond to the Kc2 of **2a** (0.039), which is indeed equivalent to the single Kc value of **2b**. The experimental Kc value of **10b** is instead quite larger (0.15, see Table 1), confirming that extensive electronic interaction takes place between the two DTO ligands of **10b**. The HCl-free N-benzyl substituted dithiooxamidate ligand of **10b** has in fact less effective electron density than the equivalent HCl-free N-ethyl dithiooxamidate ligand which is present in **2b**, so a smaller electron density can be transferred via the metal center to the HCl-coordinated, otherwise equivalent, N-ethyl substituted dithiooxamide ligand in **10b** compared to **2b**. This makes the TCIP in **10b** less stable (and therefore the HCl moiety can be more easily transferred to the pyridine, yielding a higher Kc value) than in **2b**. Interestingly, if the electronic interaction between the two DTO moieties of **10b** is taken into account by considering a virtual, geometrically averaged single $\Sigma\sigma^*$ value to **10b** (this is indeed the meaning of the $\Sigma\sigma^*$ value reported for this compound in Table 1), the linear correlation in Figure 5 is followed also by **10b**. This result, indicating that R substituents which are not directly involved in the ion pairing process (for **10b**, the benzyl substituent of the dithiooxamidate ligand) affect the stability constant of remote ion-paired sites (the ethyl-substituted N atom), suggests that long-range effects can also be active in determining the stability of TCIP species.

Conclusions

The equilibrium constants of the HCl exchange reaction between Pt(II)-containing tight contact ion pairs of general formula $\{[Pt(H_2\text{-}R_2\text{-dithiooxamide})_2]^{2+}, 2Cl^-\}$ (**a**-type compounds) and pyridine have been studied. The results show that the stability of the TCIP is significantly influenced by the nature of the R substituents of the dithiooxamide (DTO) ligands. Indeed the pKc values of the above-mentioned equilibria for the variously R-substituted compounds are linearly dependent on the σ Taft parameter of the R substituents. Moreover, the splitting of the two Kc values related to successive HCl transfer reactions occurring in each **a**-type compound decreases with the σ Taft parameter, that is on the effective electron density on the nitrogen atom of the DTO ligand, involved in the transfer reaction. This effect indicates that significant electronic interaction between the two acid−base sites of the $\{[Pt(H_2\text{-}R_2\text{-dithiooxamide})_2]^{2+}, 2Cl^-\}$ compounds takes place, most likely mediated by the metal center. In agreement with such a conclusion, the single Kc value obtained for the mixed-R compound $\{[(H\text{-benzyl}_2\text{-DTO})Pt(H_2\text{-ethyl}_2\text{-DTO})]^+, Cl^-\}$ does not correspond to the expected value for HCl exchange reaction involving an ethyl-DTO ligand, but to a Kc value geometrically averaged between ethyl- and benzyl-substituted DTO ligands. In particular, this latter result also indicates a long-range effect of the R substituent which is not directly involved in ion pairing on the TCIP stability. Finally, we proposed a parallel between splitting of Kc values in multiple TCIP systems and oxidation splitting in symmetric dinuclear metal complexes.

Altogether, our data represent an approach for investigating the stability of TCIPs and demonstrates that the equilibrium constants in the formation of multiple TCIP systems can be significantly interconnected one another and governed by parameters which can be easily tuned, such as electron density on ion pairing sites. Further work is in progress in our laboratory to investigate in detail the temperature dependence of the equilibrium constants, with the aim of obtaining thermodynamic parameters.

Experimental Section

Solvents were purified by standard procedures and distilled before the use. Secondary dithioxamides[22] and *cis*-$Pt(Me_2SO)_2Cl_2$[23] were prepared according to the literature methods. Electronic spectra were recorded with a PE Lambda35 UV VIS spectrometer. ^1H NMR and $^{13}C\{^1H\}$NMR spectra were recorded at 298 K on a Bruker ARX-300, equipped with a broadband probe operating at 300.13 and 75.56 MHz, respectively. Chemical shifts (δ, ppm) were referred to $SiMe_4$. Details on the procedure used to determine the equilibrium constants Kc are given in the Supporting Information.

Preparation of Compounds. $\{[Pt(H_2R_2DTO)_2]^{++}, 2Cl^-\}$, **a**-type **1a**−**9a** compounds have been prepared according to reported general procedures.[8,9] Characterization of **1a**, **5a**, **6a**, and **7a** have been already reported.[8,9] Characterization of new compounds is as follows:

2a. ^1H NMR (300.13 MHz, $CDCl_3$, room temperature): δ 13.55 (bs, N−H); 3.81 (q, N−CH_2−CH_3, $^3J = 7.2$); 1.38 (t, N−CH_2−CH_3, $^3J = 7.2$). $^{13}C\{^1H\}$NMR (75.48 MHz, $CDCl_3$, room temperature) δ 184.00 (*C*S); 45.00 (N−*C*H_2−CH_3); 12.18 (N−CH_2−*C*H_3). Analysis: calculated for $C_{12}H_{24}N_4S_4Cl_2Pt$ (MW 618.59): C, 23.30; H, 3.91; N, 9.06. Found: C, 23.23; H, 3.99; N, 8.92. Yield 89%.

3a. ^1H NMR (300.13 MHz, $CDCl_3$, room temperature): δ 13,37 (bs, N−*H*); 3.70 (t, N−CH_2−CH_2−CH_3, $^3J = 7.3$); 1.98 (m, N−CH_2−CH_2−CH_3); 1.06 (t, N−CH_2−CH_2−*C*H_3,

(21) (a) McConnell, H. H. *J. Chem. Phys.* **1961**, *35*, 508. (b) Lambert, C.; Nöll, G. *J. Am. Chem. Soc.* **1999**, *121*, 8434. (c) Demadis, K. D.; Hartshorn, C. M.; Meyer, T. *J. Chem. Rev* **2001**, *101*, 2655. (d) Paddon-Row, M. N. In *Electron Transfer in Chemistry* (Ed.: Balzani, V.), Wiley-VCH, Weinheim, 2001, Vol. *3*, p. 179. (e) Brunschwig, B. S.; Creutz, C.; Sutin, N. *Chem. Soc. Rev.* **2002**, *31*, 168.

(22) Hurd, R. N.; De La Mater, G.; McElheny, C. G.; Turner, R. J.; Vallingford, V. H. *J. Org. Chem.* **1961**, *26*, 3980.

(23) Kukushkin, Y. N.; Viaz'menskii, Y. E.; Zorina, L. I.; Pazhukina, Y. L. *Russ. J. Inorg. Chem.* **1968**, 13.

^3J = 7.3). $^{13}C\{^1H\}$NMR (75.48 MHz, $CDCl_3$, room temperature) δ 183.7 (*C*S); 51.65 (N−*C*H_2−CH_2−CH_3); 20.53 (N−CH_2−*C*H_2−CH_3); 11.77 (N−CH_2−CH_2−*C*H_3). Analysis: calculated for $C_{16}H_{32}N_4S_4Cl_2Pt$ (MW 674.70): C, 28.48; H, 3.91; N, 9.06. Found: C, 28.39; H, 3.81; N, 9.16. Yield 85%.

4a. ^1H NMR (300.13 MHz, $CDCl_3$, room temperature): δ 13.57 (bs, N−*H*); 4.45 (seven lines, N−C*H*$(CH_3)_2$ ^3J = 6.45); 1.57 (d, N−CH(C*H*$_3)_2$, ^3J = 6.45). $^{13}C\{^1H\}$NMR (75.48 MHz, $CDCl_3$, room temperature) δ 185.00 (*C*S); 54.03 (N−*C*H$(CH_3)_2$); 20.17 (N−CH(*C*$H_3)_2$). Analysis: calculated for $C_{16}H_{32}N_4S_4Cl_2Pt$ (MW 674.70): C, 28.48; H, 3.91; N, 9.06. Found: C, 28.53; H, 3.82; N, 8.97. Yield 78%.

8a. ^1H NMR (300.13 MHz, $CDCl_3$, room temperature): δ 13,40 (bs, N−*H*); 7.20−7.33 (m, N−CH_2−CH_2−C_6H_5); 3.95 (t, N−CH_2−CH_2−C_6H_5, ^3J = 7.7); 3.25 (t, N−CH_2−CH_2-C_6H_5, ^3J=7.7). $^{13}C\{^1H\}$NMR (75.48 MHz, $CDCl_3$, room temperature) δ 184.2 (*C*S); 123.4, 131.0, 137.3, 146.9 (N−CH_2−CH_2−*C*$_6H_5$); 51.00 (N−*C*H_2−CH_2−); 33.28 (N−CH_2−*C*H_2−C_6H_5). Analysis: calculated for $C_{36}H_{40}N_4S_4Cl_2Pt$ (MW 922.98): C, 46.84; H, 4.37; N, 6.07. Found: C, 46.61; H, 4.42; N, 6.14. Yield 86%.

9a. ^1H NMR (300.13 MHz, $CDCl_3$, room temperature): δ 13.3 (bs, N−*H*); 6.06 (m, N−CH_2−C*H*=CH_2); 5.45 (d, N−CH_2−CH=$CH_{trans}H_{cis}$, ^3J = 10.0); 5.54 (d, N−CH_2−CH=C$H_{trans}H_{cis}$, ^3J = 17.0); 4.39 (d, N−CH_2-CH=CH_2, ^3J=6). $^{13}C\{^1H\}$NMR (75.48 MHz, $CDCl_3$, room temperature) δ 184.00 (*C*S); 128.24 (N−CH_2−*C*H=CH_2); 121.42 (N−CH_2−CH=*C*H_2); 51.80 (N−*C*H_2−CH=CH_2). Analysis: calculated for $C_{16}H_{24}N_4S_4Cl_2$-Pt(MW 666.66): C, 28.83; H, 3.63; N, 8.40. Found: C, 28.72; H, 3.56; N, 9.51. Yield 91%.

{[(HR$_2$DTO)Pt(H$_2$R$_2$DTO)]$^+$,Cl$^-$}, b-Type Compounds. General Method. One mmol of *cis*-Pt$(Me_2SO)_2Cl_2$ was suspended in chloroform (150 mL) together with 2 g of $NaHCO_3$. The equivalent quantity (1 mmol) of the desired dithiooxamide was added in small amount to this mixture which becomes orange within a few minutes. The mixture was allowed to stand for 1 h. After this time $NaHCO_3$ was removed by filtration. To the orange filtrate 1 mmol of dithiooxamide was added. The solution turned purple within few minutes. After standing (1 h) the purple solution was concentrated to a small volume. Petroleum ether was added and {[(H-R_2-DTO)Pt(H$_2$-R_2-DTO)$_2$]$^+$, Cl^-} precipitated as a dark purple powder.

Compound **5b** has been already reported.[9] Characterization data for the new compounds are as follows:

1b. ^1H NMR (300.13 MHz, $CDCl_3$, room temperature): δ 13.4 (bs, N−*H*); 3.39 (s, N−CH_2−). $^{13}C\{^1H\}$NMR (75.48 MHz, $CDCl_3$, room temperature) δ 35.80 (N−*C*H_3). Analysis: calculated for $C_8H_{15}N_4S_4ClPt$ (MW 526.03): C, 18.27; H, 2.87; N, 10.65. Found: C, 18.39; H, 2.78; N, 10.78. Yield 82%.

2b. ^1H NMR (300.13 MHz, $CDCl_3$, room temperature): δ 13.21 (bs, N−H): 3.76 (q, N−CH_2−CH_3, ^3J = 7.2); 1.38 (t, N−CH_2−CH_3, ^3J = 7.2). $^{13}C\{^1H\}$NMR (75.48 MHz, $CDCl_3$, room temperature): δ 44.55 (N−*C*H_2−CH_3); 12.51 (N−CH_2−*C*H_3). Analysis: calculated for $C_{12}H_{23}N_4S_4ClPt$ (MW 582.13): C, 24.76; H, 3.98; N, 9.62. Found: C, 24.61; H, 4.05; N, 9.53. Yield 77%.

3b. ^1H NMR (300.13 MHz, $CDCl_3$, room temperature): δ 13.25 (bs, N*H*); 3.70 (t, N−CH_2−CH_2−CH_3, ^3J = 7.3); 1.98 (m, N−CH_2−CH_2−CH_3); 1.06 (t, N−CH_2−CH_2−CH_3, ^3J = 7.3). $^{13}C\{^1H\}$NMR (75.48 MHz, $CDCl_3$, room temperature): δ 51.30 (N−*C*H_2−CH_2−CH_3); 21.00 (N−CH_2−*C*H_2−CH_3); 11.80 (N−CH_2−CH_2−*C*H_3). Analysis: calculated for $C_{16}H_{31}N_4S_4ClPt$ (MW 638.24): C, 30.11; H, 4.89; N, 8.78. Found: C, 29.06; H, 4.93; N, 8.68. Yield 88%.

4b. ^1H NMR (300.13 MHz, $CDCl_3$, room temperature): δ 13.5 (bs, N−*H*); 4.42 (seven lines, N−C*H*$(CH_3)_2$ ^3J = 6.7); 1.43 (d, N−CH(C*H*$_3)_2$, ^3J = 6.7). $^{13}C\{^1H\}$NMR (75.48 MHz, $CDCl_3$, room temperature): δ 56.04 (N−*C*H$(CH_3)_2$); 21.80 (N−CH-(*C*$H_3)_2$). Analysis: calculated for $C_{16}H_{31}N_4S_4ClPt$ (MW 638.24): C, 30.11; H, 4.89; N, 8.78. Found: C, 30.25; H, 4.72; N, 8.88. Yield 84%.

6b. ^1H NMR (300.13 MHz, $CDCl_3$, room temperature): δ 13.0 (N−*H*); 4.06 (m, N−C$H_2$$(CH_2)_5$); 1.3−2.12 (m, N−$CH_2$-($CH_2$)$_5$). $^{13}C\{^1H\}$NMR (75.48 MHz, $CDCl_3$, room temperature): δ 59.40 (m, N−C$H_2$$(CH_2)_5$); 24.80, 29.90, 31.50 (N−CH_2(*C*H_2)$_5$). Analysis: calculated for $C_{32}H_{55}N_4S_4ClPt$ (MW 854.60): C, 44.97; H, 6.49; N, 6.55. Found: C, 45.11; H, 6.52; N, 6.43. Yield 90%.

7b. ^1H NMR (300.13 MHz, $CDCl_3$, room temperature): δ 13.50 (bs, N−*H*); 7.31−7.46 (m, N−CH_2−C_6H_5); 4.86 (s, N−CH_2-C_6H_5). $^{13}C\{^1H\}$NMR (75.48 MHz, $CDCl_3$, room temperature): δ 128.35, 128.90, 134.30 (N−CH_2−*C*$_6H_5$); 52.90 (N−*C*H_2−C_6H_5). Analysis: calculated for $C_{32}H_{31}N_4S_4ClPt$ (MW 830.41): C, 46.28; H, 3.76; N, 6.45. Found: C, 46.13; H, 3.70; N, 6.52. Yield 80%.

8b. ^1H NMR (300.13 MHz, $CDCl_3$, room temperature): δ 13,28 (bs, N−*H*); 7.206−7.332 (m, N−CH_2−CH_2−*C*$_6H_5$); 3.86 (t, N−CH_2−CH_2−C_6H_5, ^3J = 7.0); 3.022 (t, N−CH_2−CH_2−C_6H_5, ^3J=7.0). $^{13}C\{^1H\}$NMR (75.48 MHz, $CDCl_3$, room temperature): δ 126.61, 128.65, 128.67, 138.67 (N−CH_2−CH_2−*C*$_6H_5$); 50.40 (N−*C*H_2−CH_2−C_6H_5); 34.90 (N−CH_2−*C*H_2−C_6H_5). Analysis: calculated for $C_{36}H_{39}N_4S_4ClPt$ (MW 886.52): C, 48.77; H, 4.43; N, 6.32. Found: C, 48.90; H, 4.33; N, 6.41. Yield 83%.

9b. ^1H NMR (300.13 MHz, $CDCl_3$, room temperature): δ 13.3 (bs, N*H*); 6.05 (m, N−CH_2−C*H*=CH_2); 5.39 (d, N−CH_2−CH=C$H_{trans}H_{cis}$, ^3J = 17.0); 5.34 (d, N−CH_2−CH=$CH_{trans}H_{cis}$, ^3J = 10.0); 4.31 (d, N−CH_2-CH=CH_2, ^3J = 6). $^{13}C\{^1H\}$NMR (75.48 MHz, $CDCl_3$, room temperature): δ 130.90 (N−CH_2−*C*H=CH_2); 119.60 (N−CH_2−CH=*C*H_2); 51.70 (N−*C*H_2−CH=CH_2). Analysis: calculated for $C_{16}H_{234}$-N_4S_4ClPt (MW 630.17): C, 30.49; H, 3.68; N, 8.89. Found: C, 30.51; H, 3.77; N, 8.71. Yield 77%.

{[H(ethyl)$_2$DTO)Pt(H$_2$(benzyl)$_2$DTO)]$^+$,Cl$^-$} (10b). A 1 mmol portion of *cis*-Pt$(Me_2SO)_2Cl_2$ was suspended in chloroform (150 mL) together with 2 g of $NaHCO_3$. The equivalent quantity (1 mmol) of the diethyldithiooxamide was added in small amount to this mixture which became orange within a few minutes. The mixture was allowed to stand for 1 h. After this time $NaHCO_3$ was removed by filtration. To the orange filtrate 1 mmol of dibenzyldithiooxamide was added. The solution turned purple within few minutes. After standing (1 h) the purple solution was concentrated to a small volume. Petroleum ether was added, and {[(H(ethyl)$_2$DTO)Pt(H$_2$(benzyl)$_2$DTO)]$^+$, Cl^-} precipitated as a dark purple powder. ^1H NMR (300.13 MHz, $CDCl_3$, room temperature): δ 13.23 (bs, N*H*); 7.29−7.36 (m, N−CH_2−C_6H_5) 4.86 (s, N−CH_2−C_6H_5); 3.77 (q, N−CH_2−CH_3, ^3J = 7.2); 1.56 (t. N−CH_2−CH_3, ^3J = 7.2). $^{13}C\{^1H\}$NMR (75.48 MHz, $CDCl_3$, room temperature): δ 128.13, 128.30, 128.920 (N−CH_2−*C*$_6H_5$); 53.50 (N−*C*H_2−C_6H_5); 44.88 (N−*C*H_2−CH_3); 12.90 (N−CH_2−*C*H_3). Analysis: calculated for $C_{22}H_{27}N_4S_4ClPt$ (MW 706.27): C, 37.41; H, 3.85; N, 7.93. Found: C, 37.50; H, 3.72; N, 8.02. Yield 84%.

[Pt(HR$_2$DTO)$_2$], c-Type Compounds. [Pt$(HR_2DTO)_2$], **c**-type compounds have been prepared according to reported procedures.[8] Characterization data of **1c**, **4c**, **5c**, **6c**, and **7c** have been already reported. Characterization data of the new compounds are as follows:

2c. ^1H NMR (300.13 MHz, $CDCl_3$, room temperature): δ 3.67 (q, N−CH_2−CH_3, ^3J = 7.2); 1.38 (t, N−CH_2−CH_3, ^3J = 7.2). $^{13}C\{^1H\}$NMR (75.48 MHz, $CDCl_3$, room temperature): δ 179.60 (*C*S); 44.15 (N−*C*H_2−CH_3); 13.90 (N−CH_2−*C*H_3). Analysis: calculated for $C_{12}H_{22}N_4S_4Pt$ (MW 545.67): C, 26.41; H, 4.06; N, 10.27. Found: C, 26.38; H, 4.15; N, 10.11. Yield 81%.

3c. ^1H NMR (300.13 MHz, $CDCl_3$, room temperature): δ 3.59 (t, N−CH_2−CH_2−CH_3, ^3J=7.0): 1.78 (m, N−CH_2−CH_2−CH_3);

1.00 (t, N−CH_2−CH_2−CH_3, ^3J = 7.0). $^{13}C\{^1H\}$NMR (75.48 MHz, $CDCl_3$, room temperature): δ 179.83 (*C*S); 51.10 (N−*C*H_2−CH_2−CH_3); 22.09 (N−CH_2−*C*H_2−CH_3); 11.88 (N−CH_2−CH_2−*C*H_3). Analysis: calculated for $C_{16}H_{30}N_4S_4Pt$ (MW 601.78): C, 31.93; H, 5.02; N, 9.31. Found: C, 31.79; H, 5.12; N, 9.20. Yield 79%.

8c. ^1H NMR (300.13 MHz, $CDCl_3$, room temperature): δ 7.206−7.332 (m, N−CH_2−CH_2−C_6H_5); 3.86 (t, N−CH_2−CH_2−C_6H_5, ^3J = 7.0); 3.022 (t, N−CH_2−CH_2−C_6H_5, ^3J = 7.0). $^{13}C\{^1H\}$NMR (75.48 MHz, $CDCl_3$, room temperature): δ 180.00 (*C*S); 126.61, 128.65, 128.67, 138.67 (N−CH_2−CH_2−C_6H_5); 50.40 (N−*C*H_2−CH_2−C_6H_5); 34.90 (N−CH_2−*C*H_2−C_6H_5). Analysis: calculated for $C_{36}H_{38}N_4S_4Pt$ (MW 850.06): C, 50.86; H, 4.51; N, 6.59. Found: C, 51.01; H, 4.59; N, 6.51. Yield 82%.

9c. ^1H NMR (300.13 MHz, $CDCl_3$, room temperature): δ 6.04 (m, N−CH_2−C*H*=CH_2); 5.30 (d, N−CH_2−CH=C$H_{trans}H_{cis}$, ^3J = 17.1); 5.24 (d, N−CH_2−CH=$CH_{trans}H_{cis}$, ^3J = 10.2); 4.25 (d, N−CH_2-CH=CH_2, ^3J = 6). $^{13}C\{^1H\}$NMR (75.48 MHz, $CDCl_3$, room temperature): δ 180.53 (*C*S); 132.34 (N−CH_2−*C*H=CH_2); 118.23 (N−CH_2−CH=*C*H_2); 51.760 (N−*C*H_2−CH=CH_2). Analysis: calculated for $C_{16}H_{22}N_4S_4Pt$ (MW 593.71): C, 32.37; H, 3.74; N, 9.44. Found: C, 32.29; H, 3.68; N, 9.55. Yield 69%.

[(H(ethyl)$_2$DTO)Pt(H(benzyl)$_2$DTO)] (10c). To a chloroform solution (100 mL) of {[(H(ethyl)$_2$DTO)Pt(H_2(benzyl)$_2$-DTO)]$^+$,Cl^-} (compound **10b**, 0.2 mmol), 2 g of NaHCO3 were added, and the solution was kept under magnetic stirring. From the initial purple color, the solution turned red into few minutes. After removal of $NaHCO_3$ by filtration, the solution was concentrated to a small volume. Finally petroleum ether was added and [(H(ethyl)$_2$-DTO)Pt(H(benzyl)$_2$DTO)] precipitated as a red powder. ^1H NMR (300.13 MHz, $CDCl_3$, room temperature): δ 7.29−7.36 (m, N−CH_2−C_6H_5); 4.80 (s, N−CH_2−C_6H_5); 3.68 (q, N−CH_2−CH_3, ^3J = 7.3); 1.38 (t. N−CH_2−CH_3, ^3J = 7.2). $^{13}C\{^1H\}$NMR (75.48 MHz, $CDCl_3$, room temperature): δ 180.70 (*C*S); 127.80, 128.22, 128.78, 136.70 (N−CH_2−C_6H_5); 53.45 (N−*C*H_2−C_6H_5); 44.25 (N−*C*H_2−CH_3); 13.77 (N−CH_2−*C*H_3). Analysis: calculated for $C_{22}H_{26}N_4S_4Pt$ (MW 669.81): C, 39.45; H, 3.91; N, 8.36. Found: C, 39.31; H, 4.05; N, 8.27. Yield 83%.

Acknowledgment. The authors thank The University of Messina for financial support (Progetti di Ricerca di Ateneo, PRA).

Supporting Information Available: The absorption spectra of independently prepared **4a**, **4b**, and **4c** compounds. Absorption spectra changes upon pyridine addition of representative **a**-type and **b**-type compounds and relative titration curves. Description of the method used to calculate the equilibrium constants. This material is available free of charge via the Internet at http://pubs.acs.org.